Environmental Science Advances

PAPER

View Article Online
View Journal | View Issue

Cite this: *Environ. Sci.: Adv.*, 2022, **1**, 584

Molecular identification guided process design for deep removal of fluoride from electroplating effluent†

Xin Wei, [a] Nian Xu,[a] An Xu[a] and Xiaolin Zhang *[ab]

Fluoride was ubiquitous in effluents from various industries; however its specification in wastewater was poorly understood, hindering the rational design of a water defluoridation process. In this study, we developed a molecular identification method for fluoride in industrial wastewater by combining NMR analysis and chemical tests. Given the complicated composition and the huge quantity, electroplating effluents were chosen as the representative of fluoride-containing wastewater. ^{19}F NMR analysis suggested F^- and BF_4^- as the two main fluoride forms in raw wastewater and effluents from wastewater treatment sections, and chemical tests suggested F^- concentration in the effluents ranging from 5.1 to 7.3 mg L^{-1}. We also explored the adsorptive removal of BF_4^- by using the strongly basic ion exchange resin D201, *i.e.*, quaternary ammonated poly (styrene-*co*-divinylbenzene) beads. The adsorption of D201 toward BF_4^- followed pseudo-first-order kinetics ($k_1 = 2.45\ h^{-1}$) with an equilibrium time of less than 3 h. Adsorption isotherms were fitted well with the Langmuir model, with the maximum adsorption capacity of 257.25 mg g^{-1} at 298 K. D201 exhibited a greatly enhanced adsorption selectivity toward BF_4^- compared to common anions including Cl^- and SO_4^{2-}, mainly owing to the low hydration energy ($\Delta G_{hyd}^\circ = -220$ kJ mol^{-1}) of BF_4^-. In the fixed-bed mode, the D201 column could generate 850 and 460 bed volume (BV) clean water ([BF_4^-] < 1.5 mg-F/L) from synthetic and realistic electroplating effluents, respectively. The exhausted D201 column was fully refreshed with NaCl solution for five defluoridation cycles with a constant effective treatment amount of ~1400 BV.

Received 1st August 2022
Accepted 19th August 2022

DOI: 10.1039/d2va00177b

rsc.li/esadvances

Environmental significance

Fluorine-containing compounds are widely used in various industries as surface cleaners or catalysts. With the increasingly stringent regulation on surface water quality, the deep defluoridation of industrial effluents was put on the agenda. However, the current studies about water defluoridation mainly focus on removing free fluoride ions from groundwater. The knowledge about fluoride specification in wastewater is scarce, hindering the rational design of the water defluoridation process. This study reported molecular identification of fluoride in electroplating effluents by combining NMR analysis and chemical tests, as well as the removal method toward the identified fluoride compound. We believe that this study may inspire more studies on the defluoridation of various industrial wastewater.

1. Introduction

Fluoride compounds are widely used in various industries, such as metallurgy, rare earth separation, uranium separation, photovoltaic industry, lithium-ion batteries and electroplating industry, resulting in the discharge of a great deal of fluoride-containing wastewater.[1] To reduce the adverse effects on surface water, local governments in China have set increasingly stringent standards on allowable fluoride discharge levels in wastewater.[2] For instance, China has set a special fluoride emission limit of 2 mg L^{-1} in the ecological fragile area for aluminum and battery industries.[3,4] Recently, Jiangsu province has published a draft on the discharge standard of pollutants for municipal wastewater, regulating the fluoride discharge limit as 1.5 mg L^{-1}.[5] Owing to the relatively high K_{sp} values of fluoride-containing precipitants (*e.g.*, CaF_2 and AlF_3), it is rather difficult for the traditional precipitation and coagulation/flocculation techniques to reduce fluoride to such low levels under economically acceptable conditions.[6,7]

A variety of methods have been reported for advanced water defluoridation,[8–10] including adsorption and/or ion exchange, membrane separation, and enhanced coagulation.[11–14] In general, previous studies mainly focused on the removal of free fluoride ions from groundwater.[15–17] For instance, ion exchange

[a]State Key Laboratory of Pollution Control and Resource Reuse, School of Environment, Nanjing University, Nanjing 210023, China. E-mail: XLZhang@nju.edu.cn
[b]Research Center for Environmental Nanotechnology (ReCENT), Nanjing University, Nanjing 210023, China

† Electronic supplementary information (ESI) available: Tables S1–S2 and Fig. S1–S7. See https://doi.org/10.1039/d2va00177b

was among the most widely adopted methods for water defluoridation, and this process was determined by the electrostatic attraction between the positively charged functional groups of the polymeric resin and the free fluoride ions.[11] However, as one of the most electronegative elements (4.0 on the Pauling scale), fluoride is prone to form various compounds with heavy metals (*e.g.*, Al, and Fe) and some nonmetallic elements (*e.g.*, P, B, and Si).[18] More importantly, fluoride compounds were usually used as catalysts and surface cleaners in the forms of fluoroborate (BF_4^-) and fluorophosphate (PF_6^-) in industries.[19–24] For example, $NaBF_4$ was frequently used as a finishing catalyst in textile printing and dyeing industries, and as one crucial component of the electrolyte in the electroplating industry.[19–21] Similarly, $LiPF_6$ was the most important raw material in the lithium battery industry.[22–24]

In contrast to extensive studies about groundwater defluoridation, the knowledge of fluoride speciation in industrial effluents was very rare. Currently, fluoride was mainly determined by ion chromatography (IC) and ion-selective electrode (ISE), both of which produced chromatographic or potentiometric signals toward free fluoride ions.[25–27] In the past few decades, ^{19}F nuclear magnetic resonance (NMR) spectroscopy has been frequently employed to distinguish the structure of organofluoride compounds in organic synthesis and chemical biology.[28,29] The natural abundance of ^{19}F is 100%, and the sensitivity of the F nucleus is only slightly less than that of H, and thus ^{19}F NMR could detect fluorine at μM levels.[25] The resonances of fluoride compounds did not overlap with those of ^{13}C and ^{1}H, making ^{19}F NMR very promising in analyzing a complex matrix like industrial wastewater.[25] Moreover, it has been widely reported that a minor change in the chemical environment might cause significant chemical shifts of ^{19}F NMR spectra,[30,31] and therefore it is possible to identify all the fluoride compounds in industrial effluents. In spite of those merits, the attempts at employing ^{19}F NMR for the molecular identification of fluoride contaminants were rarely reported. The utilization of ^{19}F NMR for wastewater analysis was mainly hindered by the relatively low signal intensity caused by the low fluoride concentration (<10 mg L^{-1}), and the difficulty in the assignment of the NMR peaks considering the sensitivity of ^{19}F NMR to the chemical environment.

In this study, we demonstrated the applicability of ^{19}F NMR for fluoride species identification in electroplating wastewater. Electroplating effluents were employed as representative wastewater owing to the characteristics of complicated composition and huge quantity.[32,33] To better identify the fluoride species, we determined the fluoride concentration and the coexisting substances prior to NMR analysis, followed by freeze-drying to improve the NMR signal-noise ratio. Afterward, the possible fluoride species were conjectured based on the coexisting elements, and the references were prepared at the same fluoride level as the wastewater. Finally, ^{19}F NMR spectra were collected at a prolonged scan time and an increased scan number to further increase the signals. In addition to free fluoride ions, fluoroborate (BF_4^-) was found ubiquitous in the electroplating effluents. Furthermore, the practical potential of ion exchange in water decontamination from BF_4^- was systematically evaluated in terms of adsorption capacity, kinetics, selectivity, and reusability. Cyclic fixed-bed adsorption was carried out toward synthetic wastewater and realistic electroplating effluents. This study might shed light on efficient defluoridation for industrial wastewater based on molecular identification.

2. Materials and methods

2.1. Chemicals and reagents

All the reagents used in this study were of analytical pure or higher grade, and they were purchased from Sinopharm Chemical Reagent Co. Ltd (Shanghai, China). Ultrapure water with a resistivity of 18.25 MΩ cm was used to prepare all solutions. The commercial macroporous strongly basic anion exchanger D201, *i.e.*, quaternary ammoniated poly (styrene-*co*-divinylbenzene) beads with chloride as the anti-ions, was purchased from Zhengguang Industrial Co. Ltd (Hangzhou, China).

2.2. Water samples

The wastewater samples were collected from the Longxi electroplating wastewater treatment plant (LXWWT) located in Huizhou, China. Prior to discharge, the wastewater was treated according to the process flow illustrated in Fig. 1. The water for analysis was sampled from the outlet ports of coagulation, secondary sedimentation tank and biological aerated filter (BAF) sections. Besides, another wastewater sample was collected from an electroplating wastewater treatment plant (TXWWT) in Taixing City of China for comparison. All the collected samples were filtered with a 0.45 μm microfiltration membrane and stored in polyethylene bottles at 4 °C.

2.3. Molecular identification of fluoride in wastewater

The fluoride ions were determined with a potentiometer (Mettler Toledo InLab Reference Plus, Switzerland) coupled with a fluoride ISE (Mettler Toledo DX219, Switzerland) by mixing 5 mL water samples with 5 mL total ionic strength adjustment buffer (TISAB) containing 1 M NaCl, diluting to a constant volume of 25 mL, and adjusting pH to 5–6 with 0.1 M HCl and 0.1 NaOH. The wastewater samples were analyzed by ^{19}F and ^{11}B NMR (Bruker Avance III 600 MHz, USA) to reveal the potential fluoride speciation. ^{19}F NMR parameters were relaxation delay 1 s, pulse width 12, spectrometer frequency 564.63 MHz, spectral width 133 928.6 Hz, and number of scans 554. ^{11}B NMR parameters were relaxation delay 1 s, pulse width 12, spectrometer frequency 192.55 MHz, spectral width 38 461.5 Hz, and number of scans 128. Prior to analysis, fluoride in the samples was concentrated 5 times through freeze-drying. The concertation of BF_4^- was determined with a potentiometer (Mettler Toledo InLab Reference Plus, Switzerland) coupled with a fluoroborate ISE (Mettler Toledo DX287, Switzerland) by mixing 5 mL samples with 5 mL TISAB containing 0.5 M Na_2SO_4 and diluting to a constant volume of 25 mL without adjusting pH because this BF_4^- ISE works well at pH 2–12 and is hardly affected by pH changes.

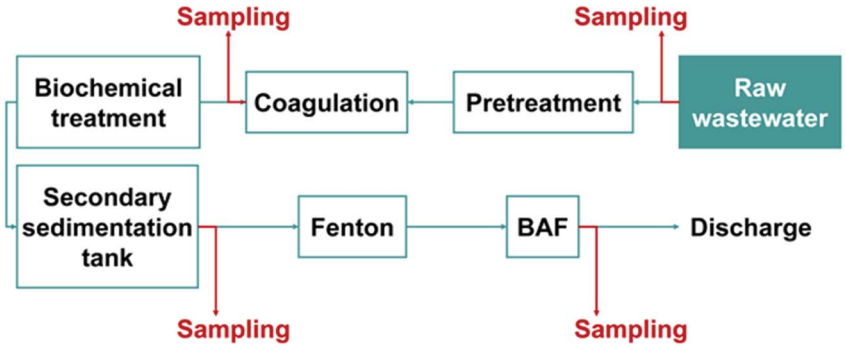

Fig. 1 Wastewater treatment process flow and sampling sites in LXWWT.

2.4. Batch adsorption experiments

Batch experiments were carried out to investigate the defluoridation capability of D201 toward synthetic water. To be specific, 0.025 g D201 was added to 50 mL $NaBF_4$ solution in a 100 mL polyethylene conical flask, followed by shaking in a thermostat shaker for 12 h to reach equilibrium. Kinetic experiments were conducted by adding 0.5 g D201 to 1 L $NaBF_4$ solution (10 mg-F/L) with or without 1000 mg L^{-1} sulfate, followed by stirring for 6 h at 298 K and initial pH = 7.0 ± 0.2. Aliquots were collected at time intervals to determine the concentration of BF_4^-. Adsorption isotherms were obtained with and without 1000 mg L^{-1} sulfate at 298, 308 and 318 K, and pH = 7.0 ± 0.2. The effects of initial pH on the adsorption of BF_4^- (10 mg-F/L) onto D201 were investigated with and without 1000 mg L^{-1} sulfate at 298 K, in a wide pH range of 3–11. The effects of competing anions on the adsorption of BF_4^- (10 mg-F/L) were tested by varying the concentration of sulfate, chloride, nitrate and perchlorate from 0 to 2000 mg L^{-1} at 298 K, and pH = 7.0 ± 0.2. Unless otherwise stated, each experiment was conducted in three replicates.

2.5. Fixed-bed experiments

Fixed-bed experiments were conducted by packing 5 mL D201 in a glass column (10 mm in diameter and 240 mm in height), and a peristaltic pump was utilized to pump the synthetic wastewater and the secondary effluent from LXWWT up-to-down through the D201 column. The flow rate was constantly kept as 20 bed volume (BV)/h, equaling an empty bed contact time (EBCT) of 3 min. After reaching adsorption saturation, D201 was regenerated by NaCl solution with a flow rate of 1 BV/h (EBCT = 6 min). The column adsorption and desorption were continuously repeated for five cycles.

2.6. Characterization and analysis

The common cations, boron, and silicate were probed by inductively coupled plasma-optical emission spectrometry (ICP-OES, Thermo Fisher iCAP7400, USA). The common anions were analyzed by IC (Thermo Fisher Dionex ICS-1100, USA). Total organic carbon (TOC) was determined by using a TOC-L_{CSH} analyzer (Shimadzu, Japan). The concertation of BF_4^- in adsorption and desorption experiments was determined with a potentiometer (Mettler Toledo InLab, Reference Plus, Switzerland) coupled with a fluoroborate ISE (Mettler Toledo DX287, Switzerland) by mixing a 5 mL sample with 5 mL TISAB containing 0.5 M Na_2SO_4 and diluting to a constant volume of 25 mL. Fourier transform infrared (FT-IR, Thermo Fisher Nicolet iS5, USA) spectroscopy was employed to detect the chemical structure of D201.

3. Results and discussion

3.1. Basic parameters of wastewater

The basic parameters of wastewater from various sections of LXWWT are described in Fig. 2a. The free fluoride ions in the raw effluent were around 25 mg L^{-1}, while the concentration declined to around 10 mg L^{-1} in the coagulation section and remained almost constant in the subsequent sections. Such results were reasonable because the polyaluminium chloride (PAC) used in the coagulation section could remove fluoride through the formation of an Al–F precipitate and/or ligand exchange with hydroxide ions. However, it has been extensively reported that coagulation cannot reduce fluoride below 1.5 mg L^{-1} under economically acceptable conditions, possibly owing to the relative high solubility product (K_{sp}) of the Al–F precipitate.[7] The evolution of pH and TOC during wastewater treatment is displayed in Fig. S1,† from which one could see that pH stayed around 7–8. The TOC in the raw water was around 50 mg L^{-1} and increased to around 70 mg L^{-1} in the coagulation effluent because of the addition of the organic coagulant (*e.g.*, polyacrylamide, PAM). After biochemical treatment and biological aerated filtering (BAF), the TOC value was reduced to below 10 mg L^{-1} again. As shown in Fig. 2b, the elements of boron (B) and magnesium (Mg) were determined to be 18–30 mg L^{-1} and 4–10 mg L^{-1} in the effluents, suggesting the possible formation of B–F and Mg–F structures in the effluent. In addition, the elements of Li, Al, Ni, and Cu were in the range of 0–1.2 mg L^{-1} (Fig. S2†).

3.2. Molecular identification of fluoride

^{19}F NMR spectroscopy was used to qualitatively identify the form of fluoride. As depicted in Fig. 2c and S3,† there were two main peaks (−121.3 and −150.7 ppm) in the wastewater sample from every section of LXWWT. Considering that the chemical

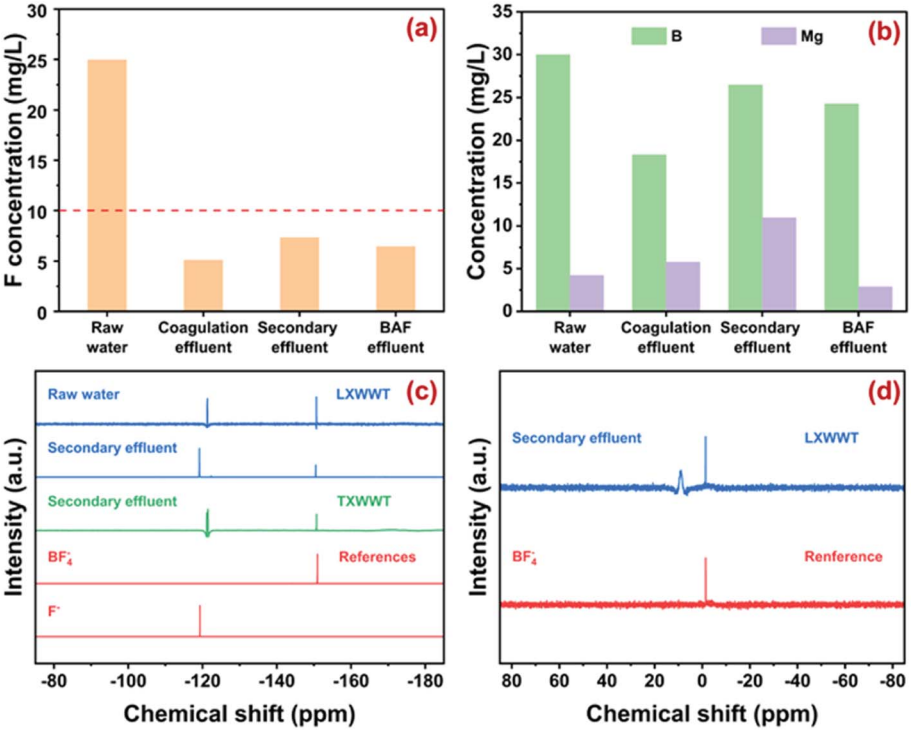

Fig. 2 Concentration of free fluoride ions (a) and elemental B and Mg (b) in the effluents from each section of LXWWT, ^{19}F NMR spectra of the effluents from LXWWT and TXWWT (c), and ^{11}B NMR spectra of the effluent from LXWWT (d).

shift of ^{19}F NMR was extremely sensitive to the surrounding chemistry such as complex configuration, solution pH, and even fluoride concentration,[30] the commercially available fluoride species including NaF and $NaBF_4$ were used as the references. Obviously, the peak at −121.3 ppm corresponded to the free fluoride ions,[31] some of which might integrate with the coexisting organic matter through electrostatic attraction or hydrogen bonding. The peak at −150.7 ppm was ascribed to fluoroborate ions (BF_4^-).[30] Moreover, the results in Fig. 2d indicated two main peaks with a chemical shift of 8.9 and −1.5 ppm[34,35] appearing in the ^{11}B NMR spectrum of the secondary effluent from LXWWT, corresponding to boric acid (H_3BO_3) and BF_4^-, respectively. The above results confirmed the presence of BF_4^- and its hydrolyzed product (H_3BO_3) in the electroplating effluent from LXWWT. Note that the possible formation of BF_3OH^- could not be ruled out, because it was rather difficult to distinguish BF_4^- from its partially hydrolyzed products [$BF_{4-x}(OH)_x^-$, $x = 1, 2, 3$] in ^{19}F and ^{11}B NMR spectra.

To verify whether BF_4^- ions were ubiquitous in electroplating wastewater, another secondary effluent sampled from TXWWT was analyzed with the ^{19}F NMR method. Similar to the wastewater sampled from LXWWT, there were also two main peaks at −121.3 and −150.7 ppm in the secondary effluent from TXWWT, attributed to free F^- ions and BF_4^- ions, respectively. Such results demonstrated that in addition to free F^-, BF_4^- might be another important species in electroplating wastewater. The presence of BF_4^- might arise from the use of fluoroboric acid (HBF_4) as an alternative to highly toxic hydrofluoric acid (HF) in the surface rinse of the plated parts. We also made a quantitative analysis of BF_4^- in the wastewater, and the results are depicted in Fig. S4.† The concentration is around 5 mg L^{-1} in the raw effluent and 2–4 mg L^{-1} in the subsequent sections, accounting for about 16% and 30% of total fluoride, confirming the significance of BF_4^- removal for deep defluoridation.

Prior to assessing the practical potential of ion exchange, the possible hydrolysis of fluoroborate was investigated. As illustrated in Fig. 3, the hydrolysis of BF_4^- followed zero-order kinetics under varying pH and temperature. With pH increasing from 3 to 11, the apparent rate constant (k_0) for BF_4^- hydrolysis decreased from 0.220 ± 0.004 to 0.100 ± 0.005 mg L^{-1} day^{-1}, while the rate constant increased from nearly zero to 0.282 ± 0.006 mg L^{-1} day^{-1} with increasing hydrolysis temperature from 277 K to 308 K. It has been extensively reported that $BF_{4-x}(OH)_x^-$ ($x = 1, 2, 3$) and H_3BO_3 were formed during the stepwise hydrolysis of BF_4^- (eqn (1)–(4)), and the generation of BF_3OH^- was the rate-limiting step. Clearly, the hydrolysis reaction was acid-catalyzed and could be accelerated with increasing temperature, in agreement with previous studies.[36–39] However, the hydrolysis of BF_4^- (initial concentration 10 mg-F/L) was still very slow and the half-life time ($t_{0.5}$) reached 90 days. In other words, there was still a considerable amount of BF_4^- (up to 80% of the total fluoride) in wastewater during the treatment process. Hence, the sequestration of BF_4^- was crucial to deep defluoridation of electroplating effluent, though adsorptive removal of BF_4^- from wastewater was rarely reported.

$$BF_4^- + H_2O \leftrightharpoons BF_3OH^- + F^- + H^+ \quad (1)$$

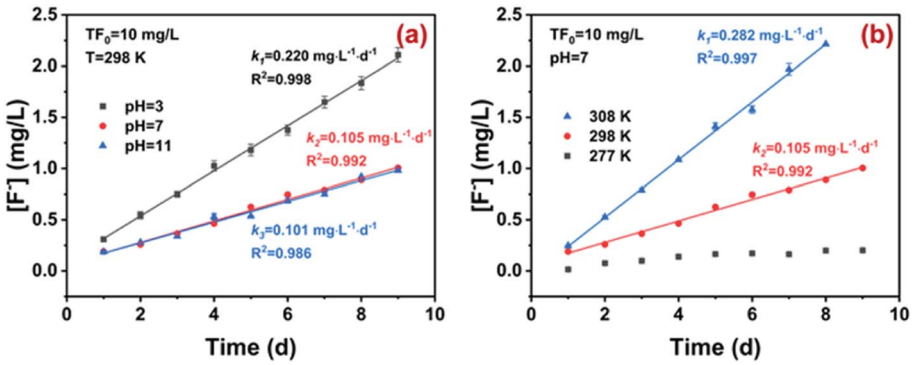

Fig. 3 Hydrolysis kinetics of BF_4^- (10 mg-F/L) at temperature = 298 K, and pH = 3, 7 and 11 (a) and at temperature = 277, 298 and 308 K, and pH = 7 (b).

$$BF_3OH^- + H_2O \leftrightharpoons BF_2(OH)_2^- + F^- + H^+ \quad (2)$$

$$BF_2(OH)_2^- + H_2O \leftrightharpoons BF(OH)_3^- + F^- + H^+ \quad (3)$$

$$BF(OH)_3^- \leftrightharpoons H_3BO_3 + F^- \quad (4)$$

3.3. Adsorption kinetics and isotherms

The strongly basic ion exchange resin D201, *i.e.*, poly (styrene-*co*-divinylbenzene) beads modified with quaternary ammonium groups, has been widely used in water soften and toxic pollutant removal,[11,40] and therefore it was selected to examine the practical potential of the ion exchange method in BF_4^- removal. The chemical structure of D201 is illustrated in Fig. S5.†

Since massive common anions often coexisted in wastewater, the adsorption kinetics of BF_4^- onto D201 was investigated in the presence or absence of sulfate (1000 mg L^{-1}). As displayed in Fig. 4a, the adsorption of D201 toward BF_4^- was very rapid in the first 30 min and reached equilibrium within 3 h. Such results were not beyond our expectation because ion exchange (electrostatic attraction) usually exhibit quick kinetics.[41,42] The presence of sulfate suppressed the adsorption kinetics and capacity of D201 toward BF_4^-, mainly owing to competition for the ion exchange sites. Both adsorption kinetics could be well fitted with a pseudo-first-order model (eqn (5)).

$$Q_t = Q_e(1 - e^{-kt}) \quad (5)$$

where Q_e (mg g^{-1}) and Q_t (mg g^{-1}) are the amount of BF_4^- adsorbed at equilibrium and at any t (h), respectively and k (g mg^{-1} h^{-1}) is the rate constant.

The first-order rate constants for the situation with and without sulfate (1000 mg L^{-1}) were calculated to be 2.45 ± 0.04 and 1.81 ± 0.04 h^{-1}, respectively, and the adsorption capacities (Q_e) were determined to be 20.91 ± 0.14 and 13.04 ± 0.06 mg g^{-1}, respectively. As a comparison, the presence of 1000 mg L^{-1} sulfate could completely screen the ion exchange capability of D201 toward other anionic pollutants including arsenate,[42] phosphate,[43] and fluoride,[11] indicating that BF_4^- might possess a relatively high ion exchange potential than the common anions. Note that the adsorption kinetics was much faster than the hydrolysis kinetics (k_0 = 0.105 mg L^{-1} day^{-1}) of BF_4^-, and thus the structural change of BF_4^- during adsorption was not considered in this study.

The FT-IR spectra of D201 after adsorption are presented in Fig. S6.† The adsorption bands at 1488 and 1477 cm^{-1} correspond to the vibration of the benzene ring, and the band at 993 cm^{-1} is assigned to the stretching vibration of C–N. These bands stem from the polystyrene skeleton and the quaternary ammonium groups of the D201 host, respectively.[44,45] A new conspicuous peak at 1049 cm^{-1} was observed, indicated the uptake of BF_4^-.

The adsorption isotherms of BF_4^- on D201 with and without sulfate (1000 mg L^{-1}) at 298 K are depicted in Fig. 4c, and the Langmuir model and Freundlich model were employed to fit the data (eqn (6) and (7)).

$$Q_e = \frac{Q_m K_L C_e}{1 + K_L C_e} \quad (6)$$

$$Q_e = K_F C_e^n \quad (7)$$

where Q_m represents the maximum adsorption capacity (mg g^{-1}), K_L is the binding constant (L mg^{-1}) which could roughly reflect adsorption affinity toward the adsorbate, and K_F (mg g^{-1})/(mg L^{-1})^n is the Freundlich constant, and n is the Freundlich intensity parameter.

Obviously, the adsorption isotherms of D201 toward BF_4^- were well fitted with the Langmuir model (R^2 = 0.99). In the presence of 1000 mg L^{-1} sulfate, the maximum adsorption capacity of D201 towards BF_4^- was calculated to be 191.04 ± 14.79 mg g^{-1}, decreased by ~25% in comparison with the value without sulfate. Adsorption isotherms were also recorded at different temperatures (298, 308 and 318 K), and the data (Fig. 4c) were well fitted with the Langmuir model (eqn (6)). The fitted parameters are listed in Table S1,† based on which one could calculate the Gibbs energy change (ΔG°), enthalpy change (ΔH°), and entropy change (ΔS°) from the classic Van't Hoff equation (eqn (8)–(10)) (Table S2†).

$$\Delta G^\circ = -RT \ln K_C \quad (8)$$

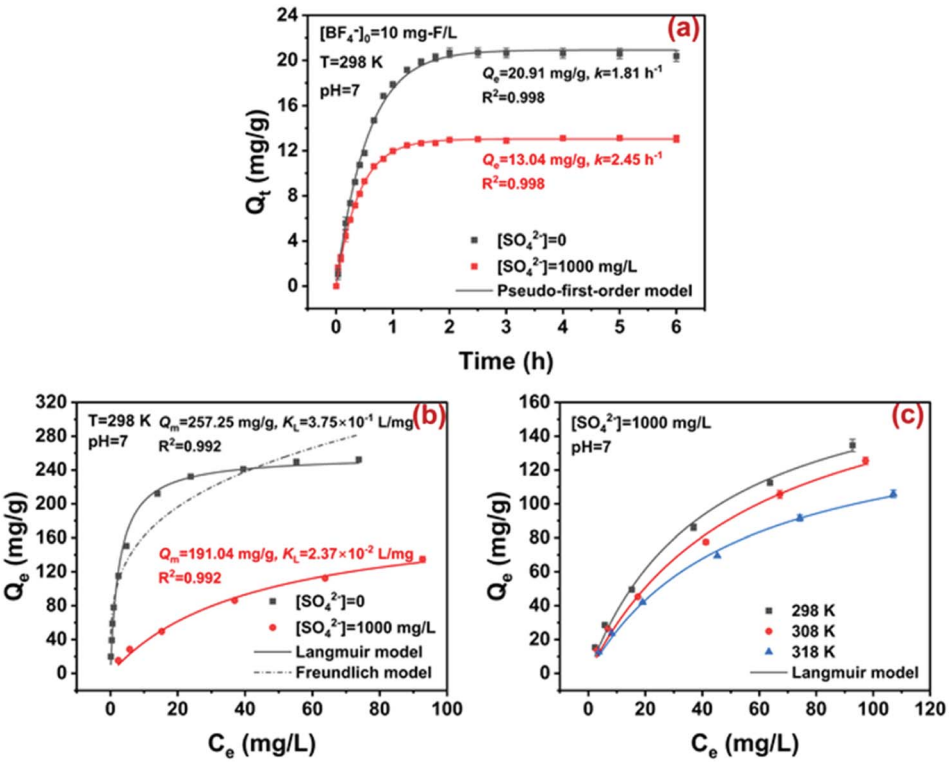

Fig. 4 Adsorption kinetics with and without 1000 mg L^{-1} sulfate ($[BF_4^-]_0 = 10$ mg-F/L, temperature = 298 K, and pH = 7) (a); adsorption isotherms with and without 1000 mg L^{-1} sulfate at temperature = 298 K and pH = 7 (b) and with 1000 mg L^{-1} sulfate at different temperature = 298, 308 and 318 K, and pH = 7 (c).

$$\ln K_C = \frac{\Delta S^\circ}{R} - \frac{\Delta H^\circ}{RT} \quad (9)$$

wherein,

$$K_C = M \times w \times 1000 \times K_L \quad (10)$$

where w represents the number (55.5) of moles of pure water per liter, and M is the atomic mass of fluorine (18.998).

It was obtained from Table S2† that ΔG° values at different temperatures were all negative and the absolute values increased with temperature, suggesting that the adsorption of BF_4^- onto D201 occurred spontaneously and the degree of spontaneity increased with temperature. The negative values ΔH° authenticate the exothermic character of adsorption,[46] consistent with the fact that the adsorption capacity declined with temperature increasing from 298 to 318 K. The positive ΔS° value indicated the increase of randomness at the solid/liquid interface after BF_4^- uptake. Obviously, the adsorption of D201 toward BF_4^- was controlled by entropic change, possibly arising from the dehydration of the hydrated BF_4^- and/or coulombic interaction between BF_4^- and the quaternary ammonium groups, as discussed below.

3.4. Effects of pH and competing anions

With pH increasing from 3 to 11, the adsorption capacity of D201 toward BF_4^- remained almost constant regardless of whether sulfate coexisted or not (Fig. 5a). As discussed above, the hydrolysis of BF_4^- was very slow and therefore it was ignored during the adsorption process. As BF_4^- existed in the form of a monovalent anion in a wide pH range (0–14), and the quaternary ammonium groups in D201 were always positively charged, the electrostatic attraction between BF_4^- and D201 was unaffected by varying pH from 3 to 11. Note that under alkaline conditions, the coexisting OH^- had minor effects on BF_4^- removal because of the relatively high hydration energy (-439 kJ mol^{-1}), as discussed below. The pH-insensitive adsorption capacity of a strongly basic ion exchange resin has been extensively reported before for fluoride[37] and nitrate.[41,46,47] As described above, the hydrolysis of BF_4^- was very slow, while the adsorption was fast. That means, during the fast process of adsorption, BF_4^- existed stably in its initial form, insensitive to pH changes. Thus, the performance was also stable at different pH, distinguished from arsenate and phosphate. Additionally, under alkaline conditions, the ion exchange of BF_4^- was hardly affected by the competing hydroxide ion because of its lower hydration energy than the latter, which was also discussed below.

The effects of common anions including chloride, nitrate, and sulfate on the adsorption capacity of D201 are depicted in Fig. 5b. Clearly, the addition of anions suppressed the adsorption of D201 toward BF_4^-, mainly because ion exchange was dominated by nonspecific electrostatic attraction.[48] Note that the anions with low hydration energy (ΔG_{hyd}°) rather than high charge density exerted strong competition for BF_4^- adsorption, *e.g.*, 10 mM sulfate with a ΔG_{hyd}° value of -1090 kJ mol^{-1} could decrease the adsorption capacity toward BF_4^- by 40%, while the

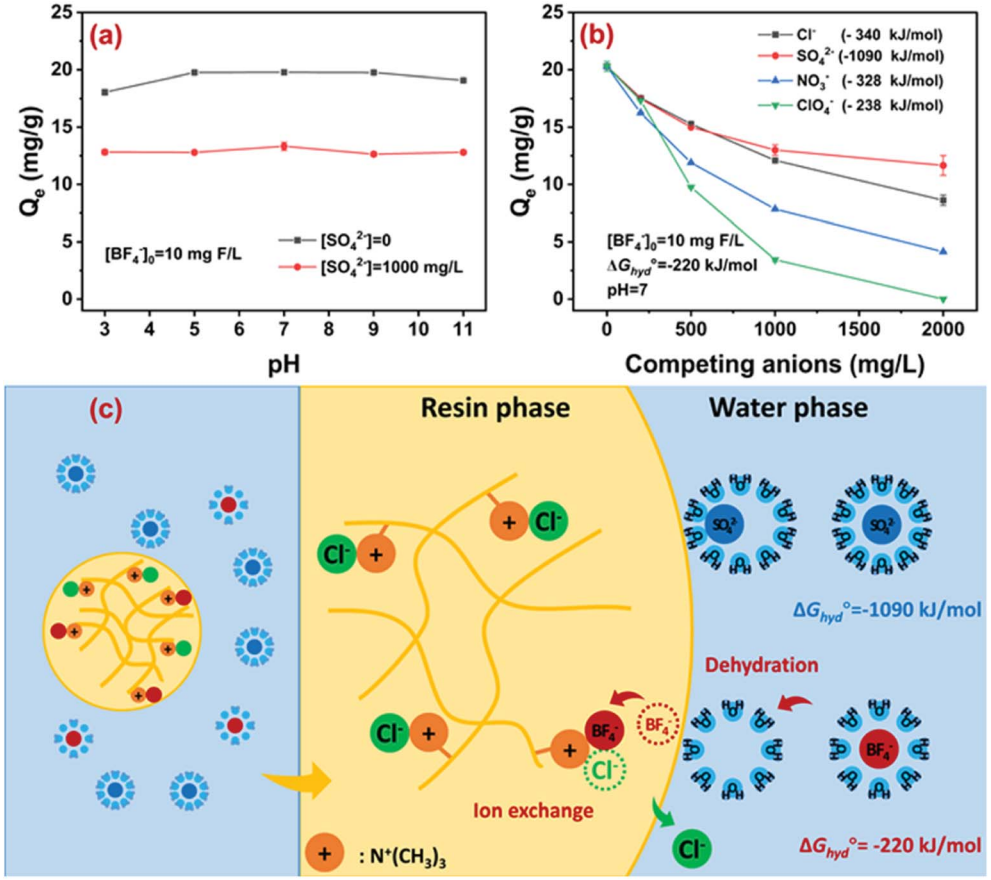

Fig. 5 Effects of pH with and without 1000 mg L^{-1} sulfate (a) and effects of competing anions at pH = 7 (b) on the adsorption of D201 toward BF_4^- (10 mg-F/L) at 298 K, and the plausible mechanism for BF_4^- removal (c).

value for 10 mM nitrate ($\Delta G_{hyd}° = -328$ kJ mol^{-1}) was 50%. As discussed above, the adsorption of BF_4^- onto D201 was controlled by entropic change, and such results illumined that the dehydration of the hydrated BF_4^- might be the dominant step determining its adsorption selectivity. Moreover, the effects of perchlorate with an approximate $\Delta G_{hyd}°$ (-238 kJ mol^{-1}) compared to BF_4^- (-220 kJ mol^{-1}) was investigated, and 10 mM perchlorate suppressed the adsorption capacity of D201 toward BF_4^- by ~86%, further demonstrating the key role of dehydration in the removal of BF_4^-. The plausible mechanism for BF_4^- removal is illustrated in Fig. 5c. The removal of BF_4^- from water was due to the electrostatic attraction by the positively charged quaternary ammonium groups. A nonspecific equilibrium exchange occurred between BF_4^- and the anti-ions (*i.e.*, Cl^-) in D201. The adsorption selectivity may depend on the hydration energy of the ions and the hydrophilicity of the resin matrix. Specifically, the ion with a lower hydration energy (*e.g.*, BF_4^-) exhibited a higher exchange potential, and the hydrophobic microenvironment could facilitate the dehydration and the subsequent ion exchange process of BF_4^-.[48]

3.5. Fixed-bed adsorption and regeneration

Given that the flow-through system has been widely adopted in practical water treatment, the column adsorption of D201 toward synthetic and real electroplating wastewater was carried out. The basic parameters of the synthetic water could be found in Fig. 6a. Negligible BF_4^- was detected in the initial 400 bed volume (BV) effluent even under strong competing conditions (1000 mg L^{-1} sulfate), thanks to the high adsorption selectivity of D201 toward BF_4^-. Afterwards, the concentration of BF_4^- increased and exceeded 10 mg-F/L at around 1500 BV. The effective treatment amount of 1500 BV was comparable with the most efficient adsorbents for the advanced removal of other toxic anions from water.[8,37–40] Our preliminary study suggested that NaCl solution (20 wt%) could regenerate the exhausted D201 efficiently in batch assays (Fig. S7†). As displayed in Fig. 6b, in the column mode, it required around 22 BV NaCl solution (20 wt%) to refresh the exhausted D201 (desorption rate $\eta \approx 90\%$), and the maximum BF_4^- concentration in the desorption effluent reached around 1300 times (1.3 g-F/L) the initial concentration in the synthetic wastewater. Cyclic column adsorption–desorption runs suggested that the effective treatment amount declined from 1500 BV to 1400 BV in the 2nd run, possibly due to the irreversible occupation of the ion exchange sites by the anions (Cl^- or BF_4^-). In the subsequent runs, the effective treatment amount always remained at around 1400 BV with a constant desorption rate (η) more than 90%, demonstrating the excellent reusability of D201 for BF_4^- removal. The column adsorption toward the real electroplating wastewater

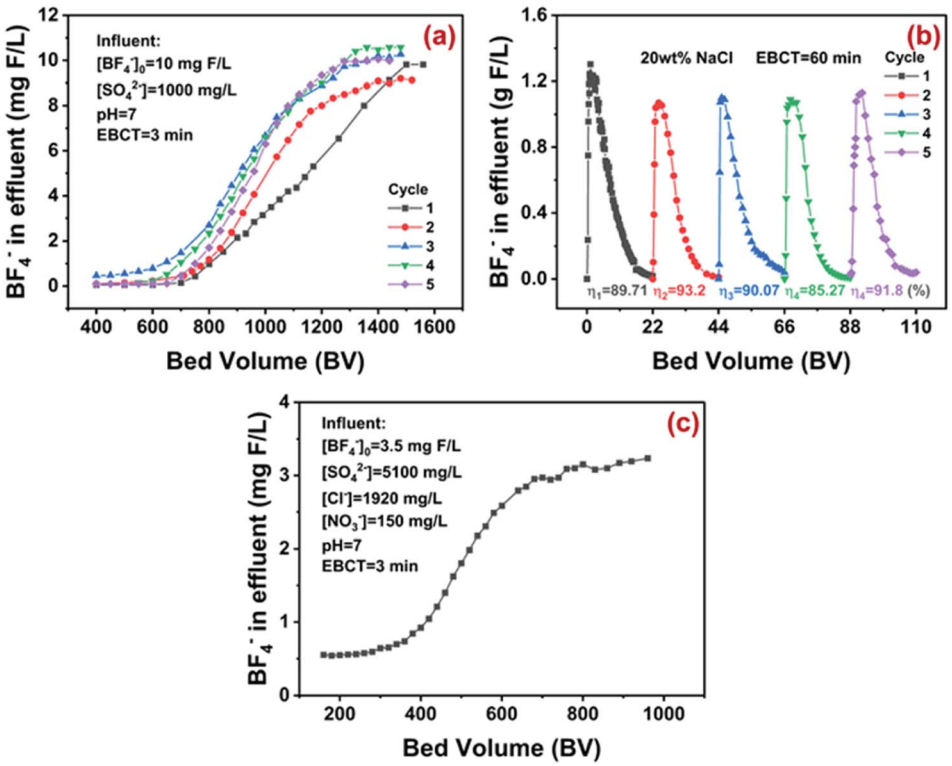

Fig. 6 Fixed-bed treatment of synthetic wastewater by the D201 column (a), cyclic column desorption with 20 wt% NaCl solution (b), and fixed-bed treatment of the real electroplating wastewater (c).

from LXWWT (the BAF effluent) is described in Fig. 6c. Obviously, there were massive sulfate, chloride, and nitrate coexisting in the real electroplating effluent, and the D201 column was still capable of purifying more than 550 BV wastewater with the BF_4^- concentration below 1.5 mg-F/L. The regeneration eluents can be recycled by adding $Ca(OH)_2$ or/and $CaCl_2$. Adding $Ca(OH)_2$ could promote the transformation of BF_4^- into F^-,[49] which can be reduced to a relatively low level (<10 mg L^{-1}) by precipitation with Ca^{2+}.[50] After solid–liquid separation, the regeneration eluents can be recycled for regeneration of the resin.

4. Conclusion

Herein, with the help of ^{19}F and ^{11}B NMR analysis, we demonstrated the ubiquitous existence of BF_4^- in electroplating effluents as a major fraction of fluoride. The possible hydrolysis of BF_4^-, which released free fluoride ions, in wastewater was confirmed to be very slow and the half-life time ($t_{0.5}$) reached 90 days. The molecular identification guided us to remove BF_4^- through ion exchange by using the commercially available strongly basic resin D201. The adsorption of D201 toward BF_4^- followed pseudo-first-order kinetics ($k_1 = 2.45\ h^{-1}$) with an equilibrium time of less than 3 h. Adsorption isotherms were fitted well with the Langmuir model, with the maximum adsorption capacity of 257.25 mg g^{-1} at 298 K. Attractively, the adsorption of D201 toward BF_4^- exhibited strong resistance against the common coexisting anions including sulfate and chloride, mainly thanks to the low hydration energy ΔG_{hyd}° (-220 kJ mol^{-1}) of BF_4^-. In the fixed-bed adsorption, the D201 column could successively produce more than 850 BV clean water with BF_4^- below 1.5 mg-F/L, and the exhausted D201 was steadily refreshed by using NaCl solution for cyclic use with only a slight decrease (~100 BV) in the effective treatment amount. Also, the D201 column exhibited satisfactory defluoridation performance toward the realistic electroplating effluent, producing more than 460 BV clean water with BF_4^- below 1.5 mg-F/L. We anticipated that this study may inspire more attempts at analyzing the fluoride species in various industrial effluents and at developing the corresponding defluoridation process for industrial effluents.

Conflicts of interest

There are no conflicts to declare.

Acknowledgements

We greatly appreciate the financial support from the Natural Science Foundation of China (Grant no. 22122604) and the Fundamental Research Funds for the Central Universities.

References

1 K. Wan, L. Huang, J. Yan, B. Ma, X. Huang, Z. Luo, H. Zhang and T. Xiao, Removal of fluoride from industrial wastewater

by using different adsorbents: A review, *Sci. Total Environ.*, 2021, **773**, 145535.
2 X.-H. Wang, X. Wang, G. Huppes, R. Heijungs and N.-Q. Ren, Environmental implications of increasingly stringent sewage discharge standards in municipal wastewater treatment plants: case study of a cool area of China, *J. Cleaner Prod.*, 2015, **94**, 278–283.
3 Minstry of ecology and environment of the PR China, Emission standard of pollutants for battery industry, GB 30484-2013, **https://www.mee.gov.cn/ywgz/fgbz/bz/bzwb/dqhjbh/dqgdwrywrwpfbz/201312/t20131227_265768.shtml**, (accessed September 2022).
4 Minstry of ecology and environment of the PR China, Emission standard of pollutants for aluminum industry, GB 25465-2010, **https://www.mee.gov.cn/ywgz/fgbz/bz/bzwb/shjbh/swrwpfbz/201010/t20101009_195339.shtml**, (accessed September 2022).
5 Department of Ecology and Environment of Jiangsu Province, PR China, Discharge standard of pollutants for municipal wastewater (Draft), **http://sthjt.jiangsu.gov.cn/art/2021/12/14/art_83848_10215706.html**, (accessed September 2022).
6 B. D. Turner, P. Binning and S. Stipp, Fluoride Removal by Calcite: Evidence for Fluorite Precipitation and Surface Adsorption, *Environ. Sci. Technol.*, 2005, **39**, 9561–9568.
7 H. Qiu, M. Ye, M.-D. Zhang, X. Zhang, Y. Zhao and J. Yu, Nano-Hydroxyapatite Encapsulated inside an Anion Exchanger for Efficient Defluoridation of Neutral and Weakly Alkaline Water, *ACS ES&T Engg*, 2021, **1**, 46–54.
8 T. A. Saleh, Protocols for synthesis of nanomaterials, polymers, and green materials as adsorbents for water treatment technologies, *Environ. Technol. Innovation*, 2021, **24**, 101821.
9 T. A. Saleh, M. Mustaqeem and M. Khaled, Water treatment technologies in removing heavy metal ions from wastewater: A review, *Environ. Nanotechnol., Monit. Manage.*, 2022, **17**, 100617.
10 T. A. Saleh, Nanomaterials: Classification, properties, and environmental toxicities, *Environ. Technol. Innovation*, 2020, **20**, 101067.
11 B. Pan, J. Xu, B. Wu, Z. Li and X. Liu, Enhanced removal of fluoride by polystyrene anion exchanger supported hydrous zirconium oxide nanoparticles, *Environ. Sci. Technol.*, 2013, **47**, 9347–9354.
12 X. Zhang, L. Zhang, Z. Li, Z. Jiang, Q. Zheng, B. Lin and B. Pan, Rational Design of Antifouling Polymeric Nanocomposite for Sustainable Fluoride Removal from NOM-Rich Water, *Environ. Sci. Technol.*, 2017, **51**, 13363–13371.
13 Y. Gan, X. Wang, L. Zhang, B. Wu, G. Zhang and S. Zhang, Coagulation removal of fluoride by zirconium tetrachloride: Performance evaluation and mechanism analysis, *Chemosphere*, 2019, **218**, 860–868.
14 Q. Zhang, S. Bolisetty, Y. Cao, S. Handschin, J. Adamcik, Q. Peng and R. Mezzenga, Selective and Efficient Removal of Fluoride from Water: In Situ Engineered Amyloid Fibril/ZrO_2 Hybrid Membranes, *Angew. Chem., Int. Ed.*, 2019, **58**, 6012–6016.
15 K. K. Yadav, S. Kumar, Q. B. Pham, N. Gupta, S. Rezania, H. Kamyab, S. Yadav, J. Vymazal, V. Kumar, D. Q. Tri, A. Talaiekhozani, S. Prasad, L. M. Reece, N. Singh, P. K. Maurya and J. Cho, Fluoride contamination, health problems and remediation methods in Asian groundwater: A comprehensive review, *Ecotoxicol. Environ. Saf.*, 2019, **182**, 109362.
16 M. Mohapatra, S. Anand, B. K. Mishra, D. Giles and P. Singh, Review of fluoride removal from drinking water, *J. Environ. Manage.*, 2009, **91**, 67–77.
17 S. Jagtap, M. K. Yenkie, N. Labhsetwar and S. Rayalu, Fluoride in drinking water and defluoridation of water, *Chem. Rev.*, 2012, **112**, 2454–2466.
18 Y. Deng, D. K. Nordstrom and R. Blaine McCleskey, Fluoride geochemistry of thermal waters in Yellowstone National Park: I. Aqueous fluoride speciation, *Geochim. Cosmochim. Acta*, 2011, **75**, 4476–4489.
19 Y. Feng, X. Jiang, Y. Chi, X. Li and H. Zhu, Volatilization Behavior of Fluorine in Fluoroborate Residue during Pyrolysis, *Environ. Sci. Technol.*, 2012, **46**, 307–311.
20 G. Shi, F. Zhang, B. Zhang, D. Hou, X. Chen, Z. Yang and S. Pan, Na2B6O9F2: A Fluoroborate with Short Cutoff Edge and Deep-Ultraviolet Birefringent Property Prepared by an Open High-Temperature Solution Method, *Inorg. Chem.*, 2017, **56**, 344–350.
21 L. E. Barrosse-Antle, A. M. Bond, R. G. Compton, A. M. O'Mahony, E. I. Rogers and D. S. Silvester, Voltammetry in Room Temperature Ionic Liquids: Comparisons and Contrasts with Conventional Electrochemical Solvents, *Chem.–Asian J.*, 2010, **5**, 202–230.
22 A. Zhao, F. Zhong, X. Feng, W. Chen, X. Ai, H. Yang and Y. Cao, Efficient and Facile Electrochemical Process for the Production of High-Quality Lithium Hexafluorophosphate Electrolyte, *ACS Appl. Mater. Interfaces*, 2020, **12**, 32771–32777.
23 N. Susarla and S. Ahmed, Estimating Cost and Energy Demand in Producing Lithium Hexafluorophosphate for Li-Ion Battery Electrolyte, *Ind. Eng. Chem. Res.*, 2019, **58**, 3754–3766.
24 Z. Xu, H. Ye, H. Li, Y. Xu, C. Wang, J. Yin and H. Zhu, Enhanced Lithium Ion Storage Performance of Tannic Acid in LiTFSI Electrolyte, *ACS Omega*, 2017, **2**, 1273–1278.
25 H. Yahyavi, M. Kaykhaii and M. Mirmoghaddam, Recent Developments in Methods of Analysis for Fluoride Determination, *Crit. Rev. Anal. Chem.*, 2016, **46**, 106–121.
26 M. S. Frant and J. W. Ross, Electrode for Sensing Fluoride Ion Activity in Solution, *Science*, 1966, **154**, 1553–1555.
27 W. R. Barnard and D. K. Nordstrom, Fluoride in precipitation—I. Methodology with the Fluoride-selective Electrode, *Atmos. Environ.*, 1982, **16**, 99–103.
28 D. Deng, P. Deng, X. Wang and X. J. S. L. Hou, Direct Determination of Sodium Fluoride and Sodium Monofluorophosphate in Toothpaste by Quantitative 19F-NMR: A Green Analytical Method, *Spectrosc. Lett.*, 2009, **42**, 334–340.

29 R. Martino, V. Gilard, F. Desmoulin and M. Malet-Martino, Fluorine-19 or phosphorus-31 NMR spectroscopy: A suitable analytical technique for quantitative in vitro metabolic studies of fluorinated or phosphorylated drugs, *J. Pharm. Biomed. Anal.*, 2005, **38**, 871–891.
30 G. Ochoa, C. D. Pilgrim, J. Kerr, M. P. Augustine and W. H. Casey, Aqueous geochemistry at gigapascal pressures: NMR spectroscopy of fluoroborate solutions, *Geochim. Cosmochim. Acta*, 2019, **244**, 173–181.
31 M. Guendouzi, J. Faridi and L. Khamar, Chemical speciation of aqueous hydrogen fluoride at various temperatures from 298.15 K to 353.15 K, *Fluid Phase Equilib.*, 2019, **499**, 112244.
32 S. Rajoria, M. Vashishtha and V. K. Sangal, Treatment of electroplating industry wastewater: a review on the various techniques, *Environ. Sci. Pollut. Res.*, 2022, DOI: **10.1007/s11356-022-18643-y**.
33 D. Konstantinos, A. Christoforidis and E. Valsamidou, Removal of nickel, copper, zinc and chromium from synthetic and industrial wastewater by electrocoagulation, *Int. J. Environ. Sci.*, 2011, **1**, 697–710.
34 E. Muetterties, *The Chemistry of Boron and its Compounds*, John Wiley & Sons, Inc., London, New York, 1967.
35 T. Onak, H. Landesman, R. Williams and I. Shapiro, The B11 Nuclear Magnetic Resonance Chemical Shifts and Spin Coupling Values for Various Compounds, *J. Phys. Chem.*, 1959, **63**, 1533–1535.
36 C. A. Wamser, Hydrolysis of Fluoboric Acid in Aqueous Solution, *J. Am. Chem. Soc.*, 1948, **70**, 1209–1215.
37 R. Mesmer and A. Rutenberg, Fluorine-19 nuclear magnetic resonance studies on fluoroborate species in aqueous solution, *Inorg. Chem.*, 1973, **12**, 699–702.
38 C. A. Wamser, Equilibria in the System Boron Trifluoride—Water at 25, *J. Am. Chem. Soc.*, 1951, **73**, 409–416.
39 J. Katagiri, T. Yoshioka and T. Mizoguchi, Basic study on the determination of total boron by conversion to tetrafluoroborate ion (BF_4^-) followed by ion chromatography, *Anal. Chim. Acta*, 2006, **570**, 65–72.
40 J. G. Cai, Y. Y. Zhang, B. C. Pan, W. M. Zhang, L. Lv and Q. X. Zhang, Efficient defluoridation of water using reusable nanocrystalline layered double hydroxides impregnated polystyrene anion exchanger, *Water Res.*, 2016, **102**, 109–116.
41 W. Yang, J. Wang, X. Shi, H. Tang, X. Wang, S. Wang, W. Zhang and J. Lu, Preferential Nitrate Removal from Water Using a New Recyclable Polystyrene Adsorbent Functionalized with Triethylamine Groups, *Ind. Eng. Chem. Res.*, 2020, **59**, 5194–5201.
42 B. Pan, Z. Li, Y. Zhang, J. Xu, L. Chen, H. Dong and W. Zhang, Acid and organic resistant nano-hydrated zirconium oxide (HZO)/polystyrene hybrid adsorbent for arsenic removal from water, *Chem. Eng. J.*, 2014, **248**, 290–296.
43 X. Zhao, Y. Zhang, S. Pan, X. Zhang, W. Zhang and B. Pan, Utilization of gel-type polystyrene host for immobilization of nano-sized hydrated zirconium oxides: A new strategy for enhanced phosphate removal, *Chemosphere*, 2021, **263**, 127938.
44 X. Zhang, P. Huang, S. Zhu, M. Hua and B. Pan, Nanoconfined Hydrated Zirconium Oxide for Selective Removal of Cu(II)-Carboxyl Complexes from High-Salinity Water via Ternary Complex Formation, *Environ. Sci. Technol.*, 2019, **53**, 5319–5327.
45 M.-y. Cong, Y.-x. Jia, H. Wang and M. Wang, Preparation of acid block anion exchange membrane with quaternary ammonium groups by homogeneous amination for electrodialysis-based acid enrichment, *Sep. Purif. Technol.*, 2020, **238**, 116396.
46 A. Sowmya and S. Meenakshi, A novel quaternized resin with acrylonitrile/divinylbenzene/vinylbenzyl chloride skeleton for the removal of nitrate and phosphate, *Chem. Eng. J.*, 2014, **257**, 45–55.
47 H. Song, Y. Zhou, A. Li and S. Mueller, Selective removal of nitrate from water by a macroporous strong basic anion exchange resin, *Desalination*, 2012, **296**, 53–60.
48 H. Zhang, A. J. Shields, N. Jadbabaei, M. Nelson, B. Pan and R. P. Suri, Understanding and modeling removalof anionic organic contaminants (AOCs) by anion exchange resins, *Environ. Sci. Technol.*, 2014, **48**, 7494–7502.
49 J. Katagiri, S. Borjigin, T. Yoshioka and T. Mizoguchi, Formation and decomposition of tetrafluoroborate ions in the presence of aluminum, *J. Mater. Cycles Waste Manage.*, 2010, **12**, 136–146.
50 K. Zhang, X. Wei, C. Ling, Z. Deng and X. Zhang, Revisiting regeneration performance and mechanism of anion exchanger-supported nano-hydrated zirconium oxides for cyclic water defluoridation, *Sep. Purif. Technol.*, 2022, DOI: **10.1016/j.seppur.2022.121906**.